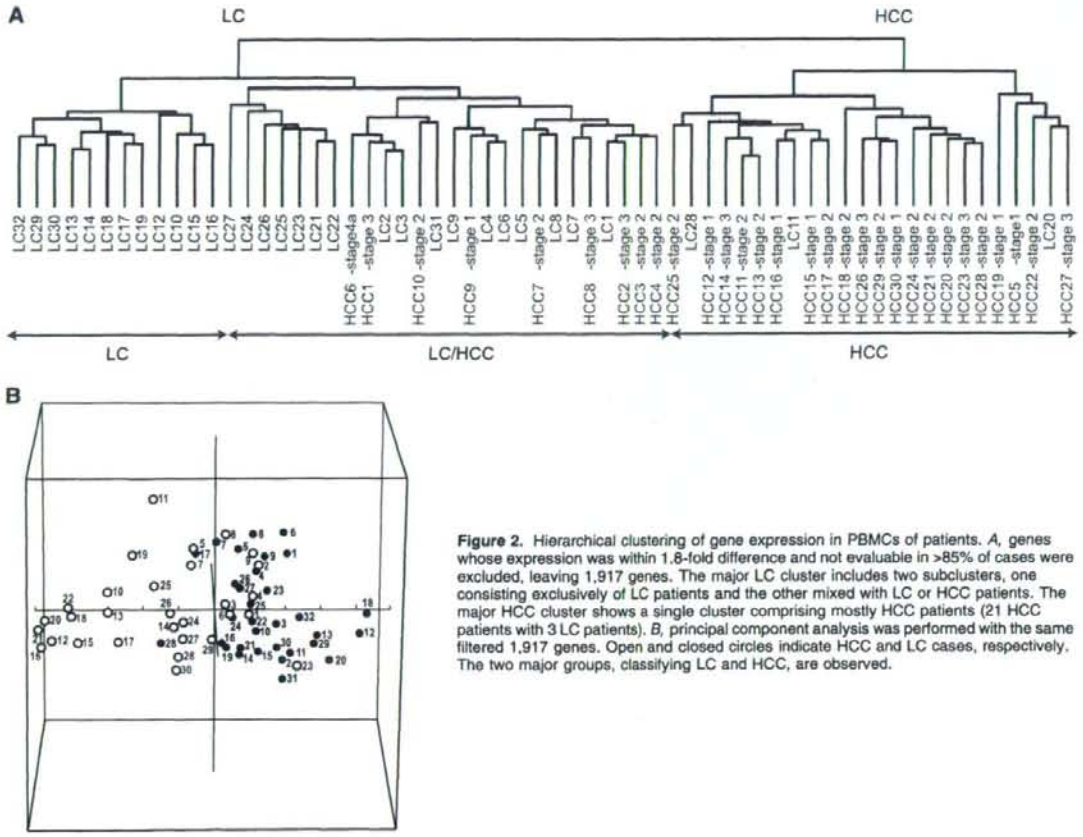

Figure 2. Hierarchical clustering of gene expression in PBMCs of patients. *A*, genes whose expression was within 1.8-fold difference and not evaluable in >85% of cases were excluded, leaving 1,917 genes. The major LC cluster includes two subclusters, one consisting exclusively of LC patients and the other mixed with LC or HCC patients. The major HCC cluster shows a single cluster comprising mostly HCC patients (21 HCC patients with 3 LC patients). *B*, principal component analysis was performed with the same filtered 1,917 genes. Open and closed circles indicate HCC and LC cases, respectively. The two major groups, classifying LC and HCC, are observed.

down-regulated genes were observed, we used MetaCore. The up-regulated genes in PBMCs from patients with HCC were involved in processes such as ubiquitin-proteasomal proteolysis (e.g., heat shock 70 kDa protein 4, ubiquitin conjugating enzymes), mRNA processing (e.g., heterogeneous nuclear ribonucleoproteins, RNA methyltransferase), antigen presentation (e.g., MHC class I polypeptide-related sequence A, B), cell cycle (e.g., HAT1, PCNA), and the response to hypoxia and oxidative stress (e.g., glutaredoxin 2, SOD2, thioredoxin; Table 3). These differentially up-regulated biological processes were also up-regulated processes in HCC-infiltrating inflammatory cells (Table 1). Thus, PBMCs from HCC patients present antigens in conditions of hypoxia and oxidative stress. Additionally, genes involved in other processes, such as apoptosis (e.g., apoptotic peptidase activating factor 1,

Table 2. Supervised learning methods for gene expression of PBMCs

Classifier category	Clinical groups	Total no. cases	No. cases misclassified	Classifier *P* values	No. genes in the classifiers ($P < 0.002$)
LC-C versus HCC	LC-C	32	8	<0.0005	1,430
	HCC	30	2		
Age (y)	>68	31	12	0.317	32
	≦68	31	16		
Gender	Male	25	15	0.178	20
	Female	37	9		
ALT (IU/L)	>50	26	20	0.82	28
	≦50	36	14		
AFP (ng/mL)	>20	29	10	0.02	301
	≦20	33	10		

Table 3. Biological processes for genes up-regulated in PBMCs of HCC patients

Biological process	−log(*P*)	Gene	ID	*t* (T/NT)	*P*	Cellular components
Ubiquitin-proteasomal proteolysis and ER	22.237	Ubiquitin specific peptidase 8	D29956	5.54	0.0000	
		Protein phosphatase 3 (formerly 2B),	NM_000945	4.90	0.0000	
		Heat shock transcription factor 2	NM_004506	4.52	0.0000	
		Heat shock 90 kDa protein 1	NM_005348	4.45	0.0000	T, M
		Ubiquitin protein ligase E3A	NM_000462	4.27	0.0001	
		Ubiquitin-conjugating enzyme E2D1	NM_003338	3.62	0.0006	M
		Phosphatidylinositol glycan, class B	NM_004855	3.57	0.0007	
		Ubiquitin-conjugating enzyme E2D2	NM_003339	3.49	0.0009	
		Ubiquitin-conjugating enzyme E2D3	NM_003340	3.18	0.0023	
		RAN binding protein 2	NM_006267	3.11	0.0029	
		Ubiquitin-conjugating enzyme E2A	NM_003336	3.09	0.0030	
		Activating transcription factor 6	NM_007348	3.03	0.0037	T, M
		Ubiquitin specific protease 7	NM_003470	2.92	0.0050	
		Heat shock 70 kDa protein 9B	NM_001746	2.91	0.0050	
		T-complex 1	NM_030752	2.76	0.0077	
		Glutaredoxin 2	NM_016066	2.70	0.0093	
		Ubiquitin-conjugating enzyme E2N	NM_003348	2.68	0.0096	
		Ubiquitin-conjugating enzyme E2 variant 2	AF049140	2.66	0.0110	
		Ubiquitin specific protease 14	NM_005151	2.20	0.0322	
		Progesterone receptor-associated p48 protein	NM_003932	2.16	0.0353	
		Heat shock 70 kDa protein 4	AB023420	2.16	0.0346	
		Ubiquitin-conjugating enzyme E2L 3	NM_003347	2.14	0.0363	
		Tenascin XB	NM_004381	2.13	0.0377	
		Ubiquitin specific peptidase 33	AB029020	2.12	0.0385	M
mRNA processing	20.087	Heterogeneous nuclear ribonucleoprotein R	NM_005826	3.90	0.0003	T
		RNA (guanine-7-) methyltransferase	NM_003799	3.29	0.0024	
		Heterogeneous nuclear ribonucleoprotein D-like	NM_031372	3.23	0.0020	
		Survival motor neuron domain containing 1	NM_005871	3.12	0.0031	
		Ribonueclease, rnase a family, 4	NM_002937	2.93	0.0052	
		Heterogeneous nuclear ribonucleoprotein A1	NM_002136	2.68	0.0094	
		Heterogeneous nuclear ribonucleoprotein K	NM_002140	2.46	0.0170	
		Heterogeneous nuclear ribonucleoprotein U	NM_031844	2.36	0.0216	
		UPF3, yeast, homologue of, A	NM_023011	2.35	0.0228	
		Alternative splicing factor	M72709	2.03	0.0471	
Antigen presentation	10.124	Janus kinase 1	NM_002227	3.38	0.0013	
		MHC, class II, DO α	NM_002119	3.09	0.0031	
		MHC, class II, DR α	NM_019111	2.67	0.0098	
		MHC class I polypeptide-related sequence B	NM_005931	2.60	0.0122	
		MHC class I polypeptide-related sequence A	NM_000247	2.26	0.0276	
		Tumor necrosis factor receptor–associated factor 6	NM_004620	2.05	0.0456	
Cell Cycle	6.185	Karyopherin (importin) β 2	NM_002270	4.32	0.0001	
		Histone acetyltransferase 1	NM_003642	4.15	0.0001	T, M
		V-myc myelocytomatosis viral oncogene homologue	NM_002467	3.57	0.0008	
		Transforming, acidic coiled-coil containing protein 1	NM_006283	3.38	0.0014	

(*Continued on the following page*)

Table 3. Biological processes for genes up-regulated in PBMCs of HCC patients (Cont'd)

Biological process	−log(*P*)	Gene	ID	*t* (T/NT)	*P*	Cellular components
		Centromere protein B, 80 kDa	X05299	3.37	0.0014	
		Conductin	AF078165	3.07	0.0032	
		Amyloid β precursor protein-binding protein 1	NM_003905	2.99	0.0040	T
		Centromere protein C 1	NM_001812	2.90	0.0054	
		Heterochromatin-like protein 1	BC000954	2.72	0.0085	
		Mature T-cell proliferation 1	BC002600	2.49	0.0154	
		Proliferating cell nuclear antigen	NM_002592	2.46	0.0166	
		CSE1 chromosome segregation 1-like	NM_001316	2.42	0.0186	M
		Karyopherin α4 (importin α3)	NM_002268	2.37	0.0209	
		Signal transducers and activators of transcription–like protein	BC010854	2.36	0.0214	
		M-phase phosphoprotein 6	NM_005792	2.34	0.0228	
		Extra spindle pole bodies homologue 1	NM_012291	2.20	0.0316	
Apoptosis	4.811	Cathepsin S	NM_004079	5.59	0.0000	M
		YME1-like 1	NM_014263	5.49	0.0000	T, M
		Cullin 5	NM_003478	4.65	0.0000	M
		Apoptotic peptidase activating factor 1	NM_001160	3.53	0.0008	
		Cullin 2	NM_003591	3.43	0.0012	M
		Amyloid β precursor protein-binding protein 1	NM_003905	2.99	0.0040	T
		Caspase 9	NM_032996	2.96	0.0044	
		F-box only protein 5	NM_012177	2.88	0.0055	
		Cullin 1	NM_003592	2.52	0.0146	
		Caspase 4	NM_001225	2.23	0.0293	
		Caspase 1	NM_033293	2.02	0.0475	
TCR signaling and immune related	5.462	Protein tyrosine phosphatase, receptor type, C	NM_002838	5.72	0.0000	
		Phosphoinositide-3-kinase, catalytic, α polypeptide	NM_006218	5.38	0.0000	
		Activating transcription factor 2	NM_001880	3.98	0.0002	
		Chemokine (c-c motif) receptor 1	NM_001295	3.90	0.0003	
		NCK adaptor protein 1	NM_006153	3.18	0.0024	
		Chemokine (c-c motif) receptor 2	NM_000647	2.78	0.0075	
		Toll-like receptor2	NM_003264	2.75	0.0078	
		Inositol 1,4,5-triphosphate receptor, type 1	NM_002222	2.24	0.0290	
		T-cell receptor α-chain	X01403	2.05	0.0452	
Response to hypoxia and oxidative stress	2.655	MAP2K1IP1	NM_021970	6.51	0.0000	
		Glutathione s-transferase θ 2	NM_000854	3.43	0.0011	
		Hypoxia-inducible factor 1, α subunit	NM_001530	2.99	0.0040	
		MAP/ERK kinase kinase 5	NM_005923	2.73	0.0086	
		Glutaredoxin 2	NM_016066	2.70	0.0093	
		Peroxiredoxin 3	NM_006793	2.68	0.0157	
		Catalase	NM_001752	2.50	0.0151	
		Plasma glutathione peroxidase 3 precursor	NM_002084	2.19	0.0329	
		Superoxide dismutase 2	NM_000636	2.10	0.0400	
		Thioredoxin	NM_003329	2.05	0.0186	

caspase 9) and T-cell receptor (TCR) signaling (e.g., CCR1, CCR2, TCR α-chain), were also up-regulated in PBMCs from patients with HCC, suggesting vulnerabilities of PBMCs and activated T-cell signaling, respectively, in HCC development.

Biological processes involving the down-regulated genes in PBMCs from patients with HCC included skeletal muscle development, the estrogen receptor 1 (ESR1) nuclear pathway, NOTCH signaling, feeding, and neurohormones signaling, neurogenesis, leptin signaling, and IL-12, IL-15, and IL-18 signaling (Supplementary Table S4), showing no obvious connection compared with the down-regulated genes in HCC-infiltrating mononuclear inflammatory cells (Supplementary Table S3). These results indicate that HCC development in cirrhotic liver can influence PBMCs, providing distinct transcriptional features of up-regulated genes even during the operable stage of HCCs.

Networks of genes commonly up-regulated or down-regulated in both PBMCs and HCC-infiltrating mononuclear inflammatory cells. Analysis of the gene expression profiles of HCC-infiltrating mononuclear inflammatory cells and PBMCs from HCC patients showed that the development of HCC altered the gene expression of local infiltrating mononuclear inflammatory cells and systemically circulating PBMCs; interestingly, the affected biological processes were largely the same. To further explore these presumed local and systemic influences resulting from HCC development, we examined how individual genes were affected by constructing a network.

We found 773 up-regulated and 750 down-regulated significant genes in HCC-infiltrating mononuclear inflammatory cells compared with noncancerous liver-infiltrating mononuclear inflammatory cells at the $P < 0.05$ level. In PBMC gene expression, we observed 2,111 up-regulated and 2,027 down-regulated genes in the PBMCs of HCC patients, compared with LC patients at the $P < 0.05$ level. Among these genes, 378 were significant in both HCC-infiltrating mononuclear inflammatory cells and PBMCs from patients with HCC (Fig. 3*A*). For these 378 genes commonly altered genes, 70% of them were up-regulated or down-regulated in both HCC-infiltrating mononuclear inflammatory cells and PBMCs from HCC patients, whereas expression of the remaining 30% of them was discordant.

We used MetaCore software to perform network construction for 172 up-regulated and 93 down-regulated genes in both HCC-infiltrating mononuclear inflammatory cells and PBMCs from HCC patients. The signal pathway network revealed three central genes, PCNA (32), SMAD3 (33), and nucleophosmin (34), which were all up-regulated in HCC-infiltrating mononuclear inflammatory cells and PBMCs from HCC patients (Fig. 3*B*). PCNA had interactions with proteasome subunit genes, PSMC2, PSMC6, PSMD12, and thioredoxin and DNA polymerase iota genes. SMAD3 was linked with cyclin-dependent kinase 7 and cyclin G_2 with various genes related to the cell cycle. Nucleophosmin was connected to ubiquitin-conjugating enzyme e2e3 and glutaredoxins. Notably, FOXP3, a marker of regulatory T cells, and Janus-activated kinase 3 (JAK3), related to interleukin signaling (35), were up-regulated and down-regulated, respectively, in HCC-infiltrating mononuclear inflammatory cells and PBMCs from HCC patients in the constructed gene network.

The network constructed for individual genes whose expression was commonly altered in HCC-infiltrating mononuclear inflammatory cells and PBMCs from HCC patients also supported a condition of HCC-related stress. The network also indicated that immune reactions in patients with HCC are complex, because down-regulated JAK3, an interleukin signaling molecule, and up-regulated FOXP3 and SMAD3, known molecules of anticancer immunity, are involved in this network. Biological processes in HCC-infiltrating mononuclear inflammatory cells and PBMCs from HCC patients also included the antigen-presentation process.

Discussion

In this study, we explored gene expression in local infiltrating mononuclear inflammatory cells in HCC and noncancerous liver tissues and in PBMCs obtained from patients with hepatitis C–related LC, with or without HCC. Gene expression profiles of HCC-infiltrating mononuclear inflammatory cells were quite distinct from those of noncancerous liver-infiltrating mononuclear inflammatory cells, showing their differing roles in anticancer immunity. We also investigated gene expression in systemically circulating PBMCs from LC-C patients with or without HCC and found that PBMC gene expression profiles from patients with or without HCC were significantly different. Intriguingly, many biological processes involving the up-regulated genes were shared between HCC-infiltrating mononuclear inflammatory cells and PBMCs from HCC patients, suggesting that the local inflammatory effect evoked by HCC development is systemically projected in the host.

Tumor-infiltrating mononuclear inflammatory cells have been investigated to examine their roles in local cancer tissues. We have selectively obtained aggregates of infiltrating mononuclear inflammatory cells in HCC and noncancerous liver tissues by LCM without contamination of carcinoma or parenchymal cells. We have shown that the process of antigen-presentation (36) is a distinguishing feature for up-regulated genes in HCC-infiltrating mononuclear inflammatory cells compared with noncancerous liver-infiltrating mononuclear inflammatory cells. Consistently, immunohistochemical staining of HCC and noncancerous liver tissues revealed that the HCC-infiltrating mononuclear inflammatory cells are primarily monocytes/macrophages, a lineage of phagocytes and antigen-presenting cells (37). Helper CD4 T cells were also found but seemed to be scattered in the HCC-infiltrating mononuclear inflammatory cells, compared with their intensive accumulation in infiltrating mononuclear inflammatory cells in noncancerous liver tissues. Correspondingly, analysis using a publicly available gene expression database of major leukocytes showed that up-regulated genes in HCC-infiltrating mononuclear inflammatory cells were primarily featured for macrophages and Th1 and Th2 CD4 cells, preconditioned with IL-12 and IL-4, respectively. These findings could be interpreted in that HCC expresses tumor-antigens (38) different from the surrounding noncancerous liver tissues; consequently, phagocytes gather in HCC tissues, take up antigens expressed by HCC tissues, and interact with CD4 cells (39). The scattered distribution and transcriptional features of both the Th1 and Th2 predisposed status of CD4 helper T cells in HCC-infiltrating mononuclear inflammatory cells suggests their versatile inflammatory status in cancer immunity, although there was no obvious shift of the Th1/Th2 balance, which is considered to be important in cancer immunity (40).

Other characteristic biological processes involving the up-regulated genes in HCC-infiltrating mononuclear inflammatory cells included the response to hypoxia and oxidative stress (41), the ubiquitin-proteasome system, cell cycle, mRNA processing, ER, and cytoplasm. The ubiquitin-proteasome system is unique to eukaryotic cells and important in maintaining the normal biological activity of cells, with pleiotropic effects in higher animals (42). The cell cycle requires precise regulation of cyclin-dependent kinase under strict control by ubiquitination and subsequent protein degradation (32). Taken together, these processes involving the up-regulated genes may reflect a protective local response of the host, corresponding to the stress environment of HCC. In this sense, the double-strand break repair gene up-regulation may be interpreted as the cells responding to maintain normal cellular activities although they are exposed to a harmful environment by the HCC (43).

The biological processes involving the up-regulated genes in PBMCs from HCC patients, compared with those from LC-C patients without HCC, were, to a substantial degree, the same, involving the up-regulated genes in HCC-infiltrating mononuclear

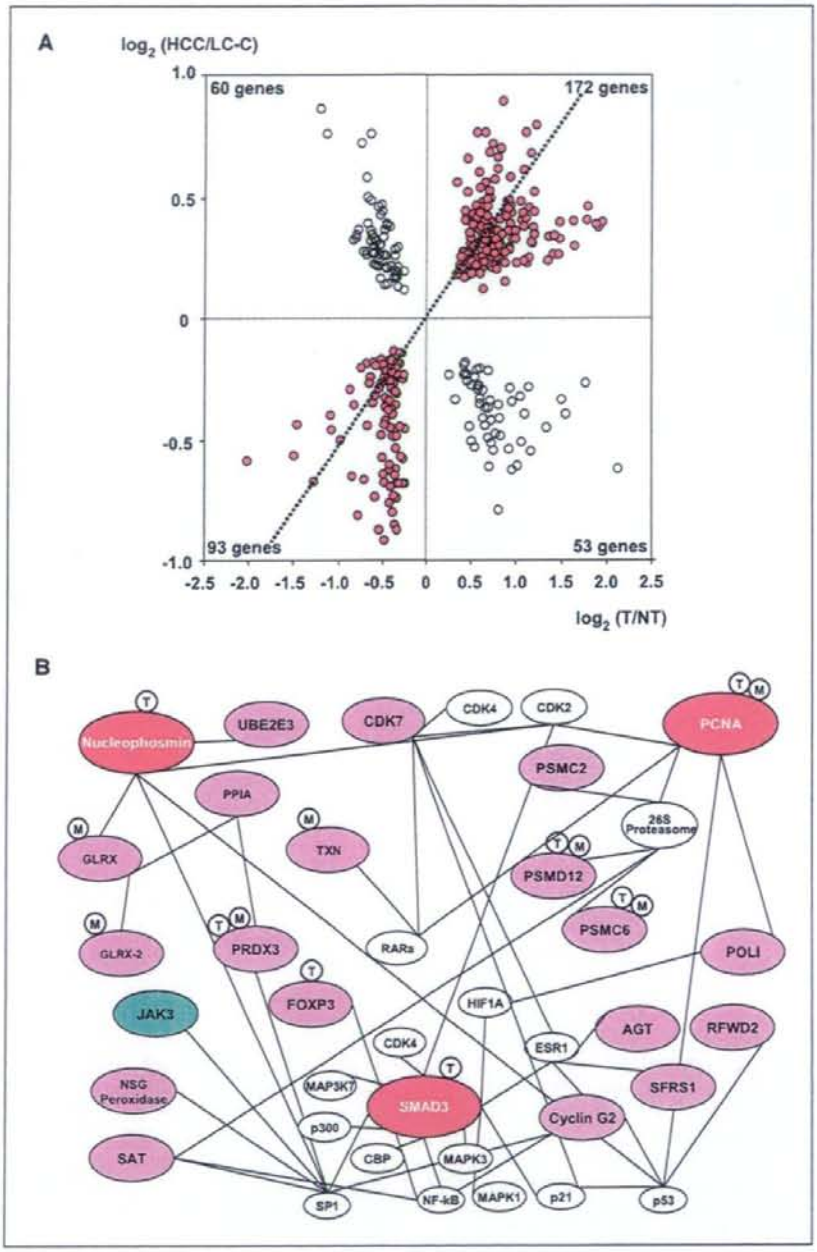

Figure 3. Features of commonly affected genes in PBMCs of HCC patients and HCC-infiltrating mononuclear inflammatory cells. *A*, scatter plots of gene expression ratios between local infiltrating mononuclear inflammatory cells and PBMCs. The axes show the binary logarithm value of the gene expression ratio of HCC-infiltrating mononuclear inflammatory cells over noncancerous liver-infiltrating mononuclear inflammatory cells on the *x* axis and the ratio of PBMCs from HCC patients over LC-C patients on the *y* axis. The right top quadrant includes 172 genes whose expression was up-regulated in HCC-infiltrating mononuclear inflammatory cells and in PBMCs from HCC patients, whereas the left bottom quadrant includes 93 genes down-regulated in both. *B*, interactive network for differentially expressed genes between PBMCs of HCC and LC-C patients and between infiltrating cells adjacent to HCC and noncancerous liver tissues. The three highlighted genes are PCNA, SMAD3, and nucleophosmin, which are related to the redox system, ubiquitin-proteasome system, and cell cycle, in addition to some immunologic gene connections. T or M at each node represent T lymphocytes or monocytes, respectively, and indicate the cell population in which each gene was expressed. The red-filled and blue-filled circles indicate up-regulation or down-regulation, respectively, in HCC-infiltrating mononuclear inflammatory cells and PBMCs from HCC patients.

inflammatory cells, such as ubiquitin-proteasomal proteolysis, ER, and cytoplasm, mRNA processing, antigen presentation, the cell cycle, and the response to hypoxia and oxidative stress. The reflection of these transcriptional features of HCC-infiltrating mononuclear inflammatory cells by PBMCs from HCC patients suggests a systemically projected influence of local HCC development, which is presumably the result of the stress environment caused by HCC and the host's reaction even when the size of the tumor is relatively small. In addition to exploring these biological processes, we also constructed networks of individual genes, the expression of which was similarly up-regulated or down-regulated, to depict commonly affected biological processes in tumor-infiltrating mononuclear inflammatory cells and PBMCs under HCC development in more detail. The networks highlighted three central genes, nucelophosmin, PCNA, and SMAD3, as up-regulated genes. They are connected to individual genes involved in ubiquitin,

proteasomes, the cell cycle, and oxidative stress (Fig. 3*B*). Interestingly, the immunologically important molecules, FOXP3 and JAK3, are in the network as up-regulated and down-regulated genes, respectively. FOXP3 is a transcriptional marker for regulatory T cells (44), and SMAD3 is also believed to be important in maintaining regulatory T cells (45). JAK3, which is associated with the interleukin receptor common γ chain (35) and is important in lymphoid development (46), was also involved in the network, suggesting that HCC influences the host immune system, which can be observed not only in HCC-infiltrating mononuclear inflammatory cells but also in the PBMCs of HCC patients. Thus, the network features of individual genes, commonly affected in HCC-infiltrating mononuclear inflammatory cells and PBMCs from HCC patients, further imply that the anticancer immunity of the host in response to HCC development involves the antigen presentation process to initiate the immune reaction.

The mechanism by which PBMCs from HCC patients reflect the transcriptional features of HCC-infiltrating mononuclear inflammatory cells requires further study. We observed that the population of CCR1-expressing and CCR2-expressing cells in PBMCs from HCC patients was higher than in those from LC-C patients. However, HCC-infiltrating mononuclear inflammatory cells did not show up-regulation of these genes. The meaning of the up-regulated CCR1 and CCR2 should be further investigated because chemokines are key molecules for the recruitment of inflammatory cells, regulating cellular adhesion and transendothelial migration, and the activation of inflammatory cells (47). The biological process of integrin-mediated cell matrix adhesion, genes involved in which were down-regulated in HCC-infiltrating mononuclear inflammatory cells, may suggest that these cells were able to remigrate into the microcirculation with the enriched blood flow in HCC tissues. The process of integrin-mediated cell matrix adhesion in HCC-infiltrating inflammatory cells may imply weaker adhesion of infiltrating mononuclear inflammatory cells to cancer tissues compared with noncancerous liver tissues (48). PBMCs are also presumed to be affected by humoral factors from HCC tissues (49). Another possibility is the presence of hematogenous spreading and circulating HCC cells because mRNA for AFP was detected in circulation (50). Because two-thirds of HCC patients enrolled for gene expression analysis of PBMCs showed serum AFP value <100, the presence of circulating HCC cells would not be evaluated by the detection of *Afp* gene expression alone. Therefore, we have examined expression of *Krt8*, *Krt18*, and *Krt19*, as well as *Afp*. Despite of the possibility of circulating cancer cells, we neither detected expression of *Afp* nor found significantly different expression of *Krt8*, *Krt18*, and *Krt19* between HCC and LC-C patients without HCC. Furthermore, genes up-regulated in HCC tissues compared with noncancerous liver tissues[3] did not correlate to up-regulated genes in PBMCs of HCC patients, indicating that different signature of gene expression in PBMCs between HCC and LC-C patients is not the reflection of the possible migrating cells from HCC tissues. In addition, all HCC cases, except for a case in gene expression analysis of PBMCs, were radiologically free of tumor thrombus in the vessel, which was indicative of microscopic invasion free or concomitant with invasion in the periphery of third or lower branch of vessels, suggesting that contribution of circulating cancer cells were presumed to be sufficiently small for the distinct difference of gene expression signature of PBMCs.

Although the number of enrolled HCC patients for analysis with local inflammatory cells was relatively small compared with the number of patients for analysis of PBMCs, our study has shown shared features of gene expression profiles of HCC-infiltrating mononuclear inflammatory cells and PBMCs from HCC patients, showing a complex immune status of the host in anticancer immunity. This finding suggests the possibility that readily accessible PBMCs can be used as a surrogate tissue to assess the local inflammatory environment surrounding cancers through examination of gene expression profiles.

Disclosure of Potential Conflicts of Interest

No potential conflicts of interest were disclosed.

Acknowledgments

Received 3/10/2008; revised 9/5/2008; accepted 9/25/2008.

The costs of publication of this article were defrayed in part by the payment of page charges. This article must therefore be hereby marked *advertisement* in accordance with 18 U.S.C. Section 1734 solely to indicate this fact.

We thank Nakamura for her invaluable contribution to this study.

[3] Unpublished data.

References

1. El-Serag HB, Mason AC. Rising incidence of hepatocellular carcinoma in the United States. N Engl J Med 1999;340:745–50.
2. Motola-Kuba D, Zamora-Valdes D, Uribe M, Mendez-Sanchez N. Hepatocellular carcinoma. An overview. Ann Hepatol 2006;5:16–24.
3. Yoshida H, Shiratori Y, Moriyama M, et al. Interferon therapy reduces the risk for hepatocellular carcinoma: national surveillance program of cirrhotic and noncirrhotic patients with chronic hepatitis C in Japan. IHIT Study Group. Inhibition of Hepatocarcinogenesis by Interferon Therapy. Ann Intern Med 1999;131:174–81.
4. Farinati F, Marino D, De Giorgio M, et al. Diagnostic and prognostic role of α-fetoprotein in hepatocellular carcinoma: both or neither? Am J Gastroenterol 2006; 101:524–32.
5. Yu P, Lee Y, Liu W, et al. Priming of naive T cells inside tumors leads to eradication of established tumors. Nat Immunol 2004;5:141–9.
6. Preynat-Seauve O, Schuler P, Contassot E, Beermann F, Huard B, French LE. Tumor-infiltrating dendritic cells are potent antigen-presenting cells able to activate T cells and mediate tumor rejection. J Immunol 2006;176: 61–7.
7. Kawata A, Une Y, Hosokawa M, Uchino J, Kobayashi H. Tumor-infiltrating lymphocytes and prognosis of hepatocellular carcinoma. Jpn J Clin Oncol 1992;22:256–63.
8. Hirano S, Iwashita Y, Sasaki A, Kai S, Ohta M, Kitano S. Increased mRNA expression of chemokines in hepatocellular carcinoma with tumor-infiltrating lymphocytes. J Gastroenterol Hepatol 2007;22:690–6.
9. Kobayashi N, Hiraoka N, Yamagami W, et al. FOXP3+ regulatory T cells affect the development and progression of hepatocarcinogenesis. Clin Cancer Res 2007;13: 902–11.
10. Williams MA, Newland AC, Kelsey SM. The potential for monocyte-mediated immunotherapy during infection and malignancy: Part I. Apoptosis induction and cytotoxic mechanisms. Leuk Lymphoma 1999;34:1–23.
11. Nakao M, Sata M, Saitsu H, et al. CD4+ hepatic cancer-specific cytotoxic T lymphocytes in patients with hepatocellular carcinoma. Cell Immunol 1997;177: 176–81.
12. Honda M, Kawai H, Shirota Y, Yamashita T, Kaneko S. Differential gene expression profiles in stage I primary biliary cirrhosis. Am J Gastroenterol 2005;100:2019–30.
13. Honda M, Yamashita T, Ueda T, Takatori H, Nishino R, Kaneko S. Different signaling pathways in the livers of patients with chronic hepatitis B or chronic hepatitis C. Hepatology 2006;44:1122–38.
14. Daiba A, Inaba N, Ando S, et al. A low-density cDNA microarray with a unique reference RNA: pattern recognition analysis for IFN efficacy prediction to HCV as a model. Biochem Biophys Res Commun 2004;315:1088–96.
15. Tateno M, Honda M, Kawamura T, Honda H, Kaneko S. Expression profiling of peripheral-blood mononuclear cells from patients with chronic hepatitis C undergoing interferon therapy. J Infect Dis 2007;195:255–67.
16. Takamura T, Honda M, Sakai Y, et al. Gene expression profiles in peripheral blood mononuclear cells reflect the pathophysiology of type 2 diabetes. Biochem Biophys Res Commun 2007;361:379–84.
17. Burczynski ME, Twine NC, Dukart G, et al. Transcriptional profiles in peripheral blood mononuclear cells prognostic of clinical outcomes in patients with advanced renal cell carcinoma. Clin Cancer Res 2005;11: 1181–9.

18. Matsui O. Imaging of multistep human hepatocarcinogenesis by CT during intra-arterial contrast injection. Intervirology 2004;47:271–6.
19. Sakai Y, Morrison BJ, Burke JD, et al. Vaccination by genetically modified dendritic cells expressing a truncated neu oncogene prevents development of breast cancer in transgenic mice. Cancer Res 2004;64:8022–8.
20. Wada Y, Nakashima O, Kutami R, Yamamoto O, Kojiro M. Clinicopathological study on hepatocellular carcinoma with lymphocytic infiltration. Hepatology 1998;27:407–14.
21. Fu J, Xu D, Liu Z, et al. Increased regulatory T cells correlate with CD8 T-cell impairment and poor survival in hepatocellular carcinoma patients. Gastroenterology 2007;132:2328–39.
22. Xu W, Roos A, Daha MR, van Kooten C. Dendritic cell and macrophage subsets in the handling of dying cells. Immunobiology 2006;211:567–75.
23. Gadola SD, Dulphy N, Salio M, Cerundolo V. Vα24-JαQ-independent, CD1d-restricted recognition of α-galactosylceramide by human CD4(+) and CD8αβ(+) T lymphocytes. J Immunol 2002;168:5514–20.
24. Feinberg H, Taylor ME, Weis WI. Scavenger receptor C-type lectin binds to the leukocyte cell surface glycan Lewis(x) by a novel mechanism. J Biol Chem 2007;282:17250–8.
25. Orabona C, Grohmann U, Belladonna ML, et al. CD28 induces immunostimulatory signals in dendritic cells via CD80 and CD86. Nat Immunol 2004;5:1134–42.
26. Demartino GN, Gillette TG. Proteasomes: machines for all reasons. Cell 2007;129:659–62.
27. Petruti-Mot AS, Earnshaw WC. Two differentially spliced forms of topoisomerase IIα and β mRNAs are conserved between birds and humans. Gene 2000;258:183–92.
28. Naryzhny SN, Desouza LV, Siu KW, Lee H. Characterization of the human proliferating cell nuclear antigen physico-chemical properties: aspects of double trimer stability. Biochem Cell Biol 2006;84:669–76.
29. Velazquez RF, Rodriguez M, Navascues CA, et al. Prospective analysis of risk factors for hepatocellular carcinoma in patients with liver cirrhosis. Hepatology 2003;37:520–7.
30. Ikeda K, Arase Y, Saitoh S, et al. Prediction model of hepatocarcinogenesis for patients with hepatitis C virus-related cirrhosis. Validation with internal and external cohorts. J Hepatol 2006;44:1089–97.
31. Tarao K, Rino Y, Ohkawa S, et al. Close association between high serum alanine aminotransferase levels and multicentric hepatocarcinogenesis in patients with hepatitis C virus-associated cirrhosis. Cancer 2002;94:1787–95.
32. Cayrol C, Ducommun B. Interaction with cyclin-dependent kinases and PCNA modulates proteasome-dependent degradation of p21. Oncogene 1998;17:2437–44.
33. Riggins GJ, Thiagalingam S, Rozenblum E, et al. Mad-related genes in the human. Nat Genet 1996;13:347–9.
34. Dhar SK, Lynn BC, Daosukho C, St Clair DK. Identification of nucleophosmin as an NF-κB co-activator for the induction of the human SOD2 gene. J Biol Chem 2004;279:28209–19.
35. Oakes SA, Candotti F, Johnston JA, et al. Signaling via IL-2 and IL-4 in JAK3-deficient severe combined immunodeficiency lymphocytes: JAK3-dependent and independent pathways. Immunity 1996;5:605–15.
36. Smyth MJ, Godfrey DI, Trapani JA. A fresh look at tumor immunosurveillance and immunotherapy. Nat Immunol 2001;2:293–9.
37. Dobrovolskaia MA, Vogel SN. Toll receptors, CD14, and macrophage activation and deactivation by LPS. Microbes Infect 2002;4:903–14.
38. Kim JW, Ye Q, Forgues M, et al. Cancer-associated molecular signature in the tissue samples of patients with cirrhosis. Hepatology 2004;39:518–27.
39. Itano AA, Jenkins MK. Antigen presentation to naive CD4 T cells in the lymph node. Nat Immunol 2003;4:733–9.
40. Budhu A, Wang XW. The role of cytokines in hepatocellular carcinoma. J Leukoc Biol 2006;80:1197–213.
41. Gerald D, Berra E, Frapart YM, et al. JunD reduces tumor angiogenesis by protecting cells from oxidative stress. Cell 2004;118:781–94.
42. Pickart CM. Back to the future with ubiquitin. Cell 2004;116:181–90.
43. Liu L, Simon MC. Regulation of transcription and translation by hypoxia. Cancer Biol Ther 2004;3:492–7.
44. Ramsdell F. Foxp3 and natural regulatory T cells: key to a cell lineage? Immunity 2003;19:165–8.
45. Fantini MC, Becker C, Monteleone G, Pallone F, Galle PR, Neurath MF. Cutting edge: TGF-β induces a regulatory phenotype in CD4+CD25- T cells through Foxp3 induction and down-regulation of Smad7. J Immunol 2004;172:5149–53.
46. Park SY, Saijo K, Takahashi T, et al. Developmental defects of lymphoid cells in Jak3 kinase-deficient mice. Immunity 1995;3:771–82.
47. Baggiolini M. Chemokines and leukocyte traffic. Nature 1998;392:565–8.
48. Leon MP, Bassendine MF, Gibbs P, Thick M, Kirby JA. Immunogenicity of biliary epithelium: study of the adhesive interaction with lymphocytes. Gastroenterology 1997;112:968–77.
49. Cao M, Cabrera R, Xu Y, et al. Hepatocellular carcinoma cell supernatants increase expansion and function of CD4(+)CD25(+) regulatory T cells. Lab Invest 2007;87:582–90.
50. Wong IH, Yeo W, Leung T, Lau WY, Johnson PJ. Circulating tumor cell mRNAs in peripheral blood from hepatocellular carcinoma patients under radiotherapy, surgical resection or chemotherapy: a quantitative evaluation. Cancer Lett 2001;167:183–91.

Available online at www.sciencedirect.com
ScienceDirect
Biochemical and Biophysical Research Communications 366 (2008) 186–192
BBRC
www.elsevier.com/locate/ybbrc

Comparative proteomic and transcriptomic profiling of the human hepatocellular carcinoma

Hirotaka Minagawa [a], Masao Honda [b,*], Kenji Miyazaki [c], Yo Tabuse [c,*], Reiji Teramoto [c], Taro Yamashita [b], Ryuhei Nishino [b], Hajime Takatori [b], Teruyuki Ueda [b], Ken'ichi Kamijo [a], Shuichi Kaneko [b]

[a] *Nano Electronics Research Laboratories, NEC Corporation, 34, Miyukigaoka, Tsukuba, Ibaraki 305-8501, Japan*
[b] *Department of Gastroenterology, Kanazawa University Graduate School of Medical Science, Kanazawa, 13-1 Takara-machi, Kanazawa 920-8641, Japan*
[c] *Bio-IT Center, NEC Corporation, 34, Miyukigaoka, Tsukuba, Ibaraki 305-8501, Japan*

Received 14 November 2007
Available online 4 December 2007

Abstract

Proteome analysis of human hepatocellular carcinoma (HCC) was done using two-dimensional difference gel electrophoresis. To gain an understanding of the molecular events accompanying HCC development, we compared the protein expression profiles of HCC and non-HCC tissue from 14 patients to the mRNA expression profiles of the same samples made from a cDNA microarray. A total of 125 proteins were identified, and the expression profiles of 93 proteins (149 spots) were compared to the mRNA expression profiles. The overall protein expression ratios correlated well with the mRNA ratios between HCC and non-HCC (Pearson's correlation coefficient: $r = 0.73$). Particularly, the HCC/non-HCC expression ratios of proteins involved in metabolic processes showed significant correlation to those of mRNA ($r = 0.9$). A considerable number of proteins were expressed as multiple spots. Among them, several proteins showed spot-to-spot differences in expression level and their expression ratios between HCC and non-HCC poorly correlated to mRNA ratios. Such multi-spotted proteins might arise as a consequence of post-translational modifications.

Keywords: Hepatocellular carcinoma; Proteome; Two-dimensional difference gel electrophoresis; Transcriptome; cDNA microarray

Hepatocellular carcinoma (HCC) is one of the most common cancers worldwide, and a leading cause of death in Africa and Asia [1]. Although several major risks related to HCC, such as hepatitis B and/or hepatitis C virus infection, aflatoxin B1 exposure, and alcohol consumption, and genetic defects, have been revealed [2], the molecular mechanisms leading to the initiation and progression of HCC are not well known. To find the molecular basis of hepatocarcinogenesis, comprehensive gene expression analyses have been done using many systems such as hepatoma cell lines and tissue samples [3,4]. Previously, we have carried out a comprehensive mRNA expression analysis using the serial analysis of gene expression (SAGE) [5] and cDNA microarray-based comparative genomic hybridization [6] to acquire the outline of gene expression profile of HCC. Although these genomic approaches have yielded global gene expression profiles in HCC and identified a number of candidate genes as biomarkers useful for cancer staging, prediction of prognosis, and treatment selection [7], the molecular events accompanying HCC development are not yet understood. In general, proteins rather than transcripts are the major effectors of cellular and tissue function [8] and it is accepted that protein expression do not always correlate with mRNA expression [9,10]. Thus, protein expression analysis, which could complement the available mRNA data, is also important to understand the molecular mechanisms of HCC.

* Corresponding authors. Fax: +81 76 234 4250 (M. Honda), +81 29 856 6136 (Y.Tabuse).
E-mail addresses: mhonda@medf.m.kanazawa-u.ac.jp (M. Honda), y-tabuse@ccd.jp.nec.com (Y. Tabuse).

0006-291X/$ - see front matter © 2007 Elsevier Inc. All rights reserved.
doi:10.1016/j.bbrc.2007.11.101

The technique of two-dimensional difference gel electrophoresis (2D-DIGE), developed by Unlu et al. [11] is one of major advances in quantitative proteomics. Several groups have recently utilized 2D-DIGE to examine protein expression changes in HCC samples [12,13], whereas reports on the analysis combining both transcriptomic and proteomic approach are rare.

In the present study, we compared quantitatively protein expression profiles of HCC to non-HCC (non-cancerous liver) samples derived from 14 patients by 2D-DIGE. We also compared the protein expression profiles of the same HCC and non-HCC samples to the mRNA profiles which have been obtained using a cDNA microarray. The expression ratios of 93 proteins showed significant correlations with the mRNA ratios between HCC and non-HCC. Proteins involved in metabolic processes showed more prominent correlation. Our study describes an outline of gene and protein expression profiles in HCC, thus providing us a basis for better understanding of the disease.

Materials and methods

Patients. A total of 14 HCC patients who had surgical resection done in the Kanazawa University Hospital were enrolled. The clinicopathological characteristics of them are shown in Table 1. The HCC samples and adjacent non-tumor liver samples were snap frozen in liquid nitrogen, and used for cDNA microarray and 2D-DIGE analysis. All HCC and non-tumor samples were histologically diagnosed and quantitative detection of hepatitis C virus RNA by Amplicore analysis (Roche Diagnostic Systems) showed positive. The grading and staging of chronic hepatitis associated with non-tumor lesion were histologically assessed according to the method described by Desmet et al. [14] and histological typing of HCC was assessed according to Ishak et al. [15]. All strategies used for gene expression and protein expression analysis were approved by the Ethical Committee of Kanazawa University Hospital.

Preparation of cDNA microarray slides. In addition to in-house cDNA microarray slides consisting of 1080 cDNA clones as previously described [6,16–18], we made new cDNA microarray slides for detailed analysis of the signaling pathway of metabolism and enzyme function in liver disease [19]. Besides cDNA microarray analysis, a total of 256,550 tags were obtained from hepatic SAGE libraries (derived from normal liver, CH-C, CH-C related HCC, CH-B, and CH-B related HCC), including 52,149 unique tags. Among these, 16,916 tags expressing more than two hits were selected to avoid the effect of sequencing errors in the libraries. From these candidate genes, 9614 non-redundant clones were obtained from Incyte Genomics (Incyte Corporation), Clontech (Nippon Becton Dickinson), and Invitrogen (Invitrogen). Each clone was sequence validated and PCR amplified by Dragon Genomics (Takara Bio), and the cDNA microarray slides (Liver chip 10k) were constructed using SPBIO 2000 (Hitachi Software) as described previously [6,16–18].

Table 1
Characteristics of patients involved in this study

Patient No.	Age	Sex[a]	Histology of non-tumor lesion[b]	Tumor histology	Viral status
1	64	M	F4A1	Moderate	HCV
2	65	M	F4A1	Well	HCV
3	48	M	F3A1	Moderate	HCV
4	69	F	F4A2	Moderate	HCV
5	66	F	F4A2	Well	HCV
6	45	M	F4A1	Well	HCV
7	75	F	F4A1	Well	HCV
8	46	M	F4A2	Moderate	HCV
9	66	M	F2A2	Well	HCV
10	75	M	F3A1	Moderate	HCV
11	67	F	F4A2	Well	HCV
12	64	M	F4A1	Moderate	HCV
13	68	M	F4A0	Well	HCV
14	74	M	F1A0	Moderate	HCV

[a] M, male; F, female.
[b] F, fibrosis; A, activity.

RNA isolation and antisense RNA amplification. Total RNA was isolated from liver biopsy samples using an RNA extraction kit (Stratagene). Aliquots of total RNA (5 μg) were subjected to amplification with antisense RNA (aRNA) using a Message AmpTM aRNA kit (Ambion) as recommended by the manufacturer. About 25 μg of aRNA was amplified from 5 μg total RNA, assuming that 500-fold amplification of mRNA was obtained. The quality and degradation of the isolated RNA were estimated after electrophoresis using an Agilent 2001 bioanalyzer. In addition, 10 μg of aRNA was used for further labeling procedures.

Hybridization on cDNA microarray slides and image analysis. As a reference for each microarray analysis, aRNA samples prepared from the normal liver tissue from one of the patients were used. Test RNA samples fluorescently labeled with cyanine (Cy) 5 and reference RNA labeled with Cy3 were used for microarray hybridization as described previously [6,16–18]. Quantitative assessment of the signals on the slides was done by scanning on a ScanArray 5000 (General Scanning) followed by image analysis using GenePix Pro 4.1 (Axon Instruments) as described previously [6,16–18].

Protein expression analysis using 2D-DIGE. Protein samples were homogenized with lysis buffer (7 M urea, 2 M thiourea, 4% w/v CHAPS, 0.8 μM aprotinin, 15 μM pepstatin, 0.1 mM PMSF, 0.5 mM EDTA, 30 mM Tris–HCl, pH 8.5) and centrifuged at 13,000 rpm for 20 min at 4 °C. The supernatants were used as protein samples. The protein concentrations were determined with a protein assay reagent (Bio-Rad). The non-HCC and HCC samples (50 μg each) labeled with either Cy3 or Cy5 according to the manufacture's manual were combined and separated on 2-DE gels together with the Cy2-labeled internal standard (IS), which was prepared by mixing equal amounts of all samples. Analytical 2-DE was performed as described previously [20] using Immobiline DryStrip (pH 3–10, 24 cm, GE Healthcare) in the first dimension and 12.5% SDS–polyacrylamide gels (24 × 20 cm) in the second dimension. Samples were run in triplicate to obtain statistically reasonable results. After scanning with a Typhoon 9410 scanner (GE Healthcare), gels were silver stained for protein identification. For protein identification, 400 μg of the IS sample was also separately run on a 2-DE gel and stained with SYPRO Ruby (Invitrogen). All analytical and preparative gel images were processed using ImageQuant (GE Healthcare) and the protein level analysis was done with the DeCyder software (GE Healthcare). To detect phosphoproteins, 400 μg of HCC and non-HCC samples were separately run on 2-DE gels and stained with ProQ Diamond (Invitrogen). After acquiring images, gels were counterstained with SYPRO Ruby to visualize total proteins as described above.

Protein identification. The excised protein spots were in-gel digested with porcine trypsin (Promega). For LC-ESI-IT MS/MS analysis using LCQ Deca XP (Thermo Electron), the digested and dried peptides were dissolved in 10 μl of 0.1% formic acid in 2% acetonitrile (ACN). The dissolved samples were loaded onto C18 silica gel capillary columns (Magic C18, 50 × 0.2 mm), and the elution from the column was directly connected through a sprayer to an ESI-IT MS. Mobile phase A was 2% ACN containing 0.1% formic acid, and mobile phase B was 90% ACN containing 0.1% formic acid. A linear gradient from 5% to 65% of concentration B was applied to elute peptides. The ESI-IT MS was operated in positive ion mode over the range of 350–2000 (m/z) and the database search was carried out against the IPI Human using MASCOT (Matrixscience). The following search parameters were used: the cutting enzyme, trypsin; one missed cleavage allowed, mass tolerance window, ±1 Da, the MS/MS tolerance window, ±0.8 Da; carbamidomethyl cystein and oxidized methionine as fixed and variable modifications, respectively.

Detection of phosphorylated peptide. Possible phosphorylation sites were investigated by MALDI-TOF-MS using monoammonium phosphate (MAP) added matrix mainly according to Nabetani et al. [21]. An additive of MAP was mixed with α-CHCA matrix solution (5 mg/mL, 0.1% TFA, 50% ACN aqueous) to 40 mM in final concentration. Tryptsin digests of the spots positively stained with ProQ were dissolved into 4 μL of 0.1% TFA, 50% ACN aqueous solution and 1 μL of the peptides solution was spotted on the MALDI target plate. After drying up, 1 μL of the MAP matrix was dropped on the dried peptide mixture. Voyager DE-STR (ABI) was used to obtain mass spectra both in negative and positive ion mode. MS peaks that had relatively stronger intensities in negative ion mode than in positive ion mode were selected as candidates for acidically modified peptides.

Results and discussion

We identified 195 spots representing 125 proteins (Suppl. Table 1) and obtained the corresponding mRNA expression data for a total of 93 proteins (149 spots) (Suppl. Table 2). These 93 proteins were classified according to their biological processes and subcellular localizations into categories described by the Gene Ontology Consortium (http://www.geneontology.org/index.shtml) and about a half of them were related to metabolic processes (Fig. 1A). It is a general agreement that proteins with extremely high or low p*I* as well as hydrophobic proteins are difficult to be detected by 2-DE. Being consistent with this notion, our analysis detected many cytoplasmic proteins (Fig. 1B). Therefore, the protein expression data presented here were biased in favor of cytoplasmic and soluble proteins. The protein expression abundance between non-HCC and HCC was calculated using the normalized spot volume, which was the ratio of spot volume relative to IS (Cy3:Cy2 or Cy5:Cy2) and we used the Student's paired *t*-test ($p < 0.05$) to select the protein spots which were expressed differentially between non-HCC and HCC, using 2-DE gel images run in triplicate. The spot volume of a multi-spotted protein was indicated as a total volume by integrating the intensities of multiple spots as was done by Gygi et al. [10]. Comparison of protein expression profiles revealed that several proteins were expressed differentially between HCC and non-HCC. Proteins whose abundances increased >2-fold or decreased <1/2 in HCC are listed in Table 2. While glutamine synthetase, vimentin, annexin A2 and aldo-keto reductase were up-regulated, carbonic anhydrase 2, argininosuccinate synthetase 1, carbonic anhydrase 1, fructose-1,6-bisphosphatase 1, and betaine-homocysteine methyltransferase were down-regulated in HCC. Up- or down-regulation of most of these proteins in HCC has been reported previously [22–27]. Up-regulation of vimentin and annexin A2, and reduced expression of carbonic anhydrase 1 and 2 was suspected to be associated with cellular motility and metastasis [23,24,26].

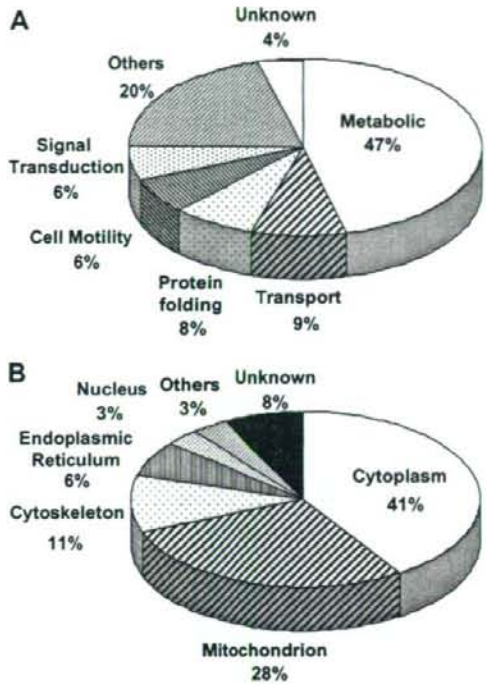

Fig. 1. Classification of identified proteins according to their cellular function (A) and subcellular localization (B).

The mRNA expression abundance was calculated from cDNA microarray data. Hierarchical clustering of

Table 2
Proteins expressed differentially between HCC and non-HCC

Spot ID	Protein name	Refseq ID	Theoretical		Fold change (HCC/non-HCC)		References
			p*I*	MW (kDa)	Protein[a]	mRNA	
1353, 1354	Glutamine synthase	NP_002056.2	6.43	42.7	2.06	3.08	[22]
1039, 1046	Vimentin	NP_003371	5.09	53.6	2.30	1.51	[23]
1716	Annexin A2	NP_001002857.1	7.57	38.8	2.57	1.82	[24]
1685, 1699	Aldo-keto reductase 1B10	NP_064695	7.12	36.2	4.29	4.73	[25]
1977	Carbonic anhydrase 2	NP_000058	6.87	29.3	0.39	0.62	[26]
1307, 1312, 1331	Argininosuccinate synthetase 1	NP_000041.2	8.08	46.8	0.41	0.30	[27]
1941	Carbonic anhydrase 1	NP_001729	6.59	28.9	0.47	1.25	[26]
1582	Fructose-1,6-bisphosphatase 1	NP_000498	6.54	37.2	0.48	0.36	
1256	Betaine-homocysteine methyltransferase	NP_001704	6.41	45.4	0.48	0.40	

[a] Integrated spot volume was used to calculate the fold change of multi-spotted proteins.

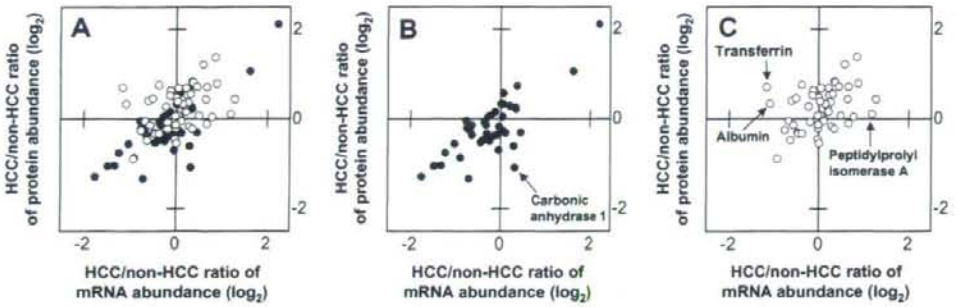

Fig. 2. Comparative analysis of protein and mRNA expression profiles between HCC and non-HCC. (A) The HCC/non-HCC ratios of averaged protein expression levels for 93 proteins were plotted against those of mRNA. Proteins related to metabolic pathways were indicated in closed circles and were shown again in (B). Proteins related to the other biochemical pathways were indicated in open circles and shown in (C). Proteins listed in Table 3 were indicated in (B) and (C). All graphs were depicted in $\log_2$ scale.

Table 3
Proteins whose expression changes between HCC and non-HCC show poor correlation to mRNA expression changes

Spot ID	Protein name	Refseq ID	Theoretical		Spot[a] Av. Ratio	Spot *p* value	Protein ratio	Micro array Av. ratio	Micro array *p* value
			*p*I	MW (kDa)					
564	Transferrin	NP_001054	6.8	79.3	2.23	0.035	1.61	0.45	3.3E−06
565					1.87	0.079			
566					2.28	0.13			
605					0.73	0.098			
1489	Albumin	NP_000468	5.9	71.3	—	0.63	1.25	0.47	2.3E−03
1941	Carbonic anhydrase 1	NP_001729	6.6	28.9	—	3.5E−03	0.47	1.25	0.39
2290	Peptidylprolyl isomerase A	NP_066953	7.7	18.1	—	5.0E−01	1.07	2.29	1.1E−01

[a] Since transferrin was detected in multiple spots, averaged ratio and spot *p* value of each spot is shown.

Table 4
Multi-spotted proteins showing spot-to-spot differences in expression level between non-HCC and HCC

Spot ID	Spot Av. ratio	Spot *p* value	Protein name	Refseq ID	Theoretical		Protein[a] ratio
					*p*I	MW (kDa)	
436	1.92	5.3E−04	Tumor rejection antigen (gp96)	NP_003290	4.8	92.7	1.2
537	0.79	0.16					
564	2.23	0.035	Transferrin	NP_001054	6.8	79.3	1.61
565	1.87	0.079					
566	2.28	0.13					
605	0.73	0.098					
1257	1.02	0.92	Fumarate hydratase	NP_000134	8.8	54.8	0.8
1261	0.6	1.3E−03					

[a] HCC/non-HCC protein ratios were calculated using integrated spot abundances.

gene expression was done with BRB-ArrayTools (http://linus.nci.nih.gov/BRB-ArrayTools.htm). The filtered data were log-transferred, normalized, centered, and applied to the average linkage clustering with centered correlation. BRB-ArrayTools contains a class comparison tool based on univariate *F* tests to find genes differentially expressed between predefined clinical groups. The permutation distribution of the *F* statistic, based on 2000 random permutations, was also used to confirm statistical significance. A *p* value of less than 0.05 for differences in HCC/non-HCC gene expression ratio was considered significant.

The average HCC/non-HCC expression ratios of the 93 proteins were plotted against the mRNA ratios in Fig. 2, where a positive value indicates increased expression in HCC and a negative ratio indicates reduced expression. The overall expression ratio of HCC/non-HCC indicated noticeable correlation between protein and mRNA

(Fig. 2A), and the Pearson's correlation coefficient for this data set (93 proteins/genes) was 0.73. Next, we divided 93 proteins into those related to metabolism and others biological processes. The HCC/non-HCC ratios of protein expression for metabolism-related proteins showed substantial correlation with those of mRNA (Fig. 2B, $r = 0.9$), whereas those of other proteins were poorly correlated (Fig. 2C, $r = 0.36$). Extreme care must be taken in a direct comparison of proteomic data with transcriptome because of multiple layers of discrepancies caused by the distinct sensitivities of cDNA array hybridization and 2-DE, the inability of a cDNA array to distinguish mRNA isoforms and post-translational modifications of proteins. Nevertheless, our results suggest that the expression of considerable portion of proteins with metabolic function listed here is regulated at transcriptional level. On the other hand, post-transcriptional and/or post-translational processes seem to be involved in the regulation of expression level for proteins with other cellular functions as a whole. Four proteins (albumin, transferrin, peptidylproryl isomerase A, and carbonic anhydrase 1) showed apparent poor correlation in protein and mRNA expression profiles (Table 3 and Fig. 2). Transcriptional control might have little effect on the expression changes of these proteins between HCC and non-HCC.

A number of proteins were expressed as multiple spots on 2-DE gels and most multi-spotted proteins showed little spot-to-spot variations in the averaged HCC/non-HCC ratio. Although we do not know how these multiple spots were generated, many of them might be due to the conformational equilibrium of proteins under electrophoresis rather than to any post-translational modifications [28]. On the other hand, the HCC/non-HCC expression ratios of several multi-spotted proteins varied from spot to spot, and three proteins (transferrin, fumarate hydratase, and tumor rejection antigen gp96) were categorized as these multi-spotted proteins (Table 4).

For example, gp96 was detected in two spots (spot #436 and 537) with distinct molecular mass and p*I* and they showed different HCC/non-HCC expression ratio (Fig. 3A and B and Table 4). The expression of these two isoforms was observed to change in the opposite direction between non-HCC and HCC: #436 was up-regulated in HCC (HCC/non-HCC ratio: 1.96) while #537 was down-regulated (HCC/non-HCC ratio: 0.79) (Table 4 and Fig. 3C and D). Gp96 is a glycoprotein present in endoplasmic reticulum and is supposed to function as a molec-

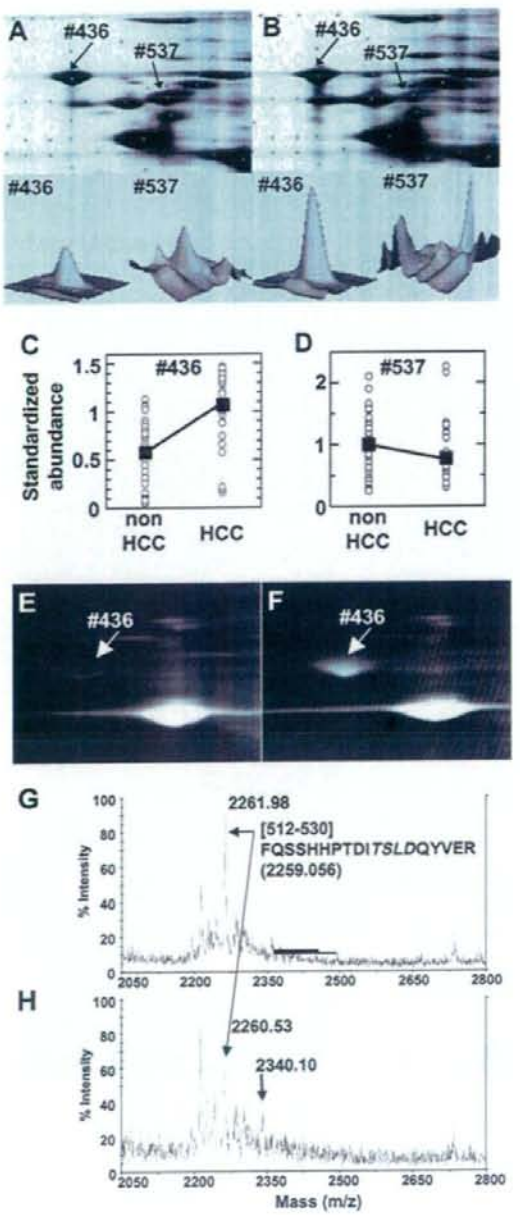

Fig. 3. Comparison of expression profiles of two gp96 spots between HCC and non-HCC. The expression profile and phosphorylation of tumor rejection antigen gp96 in HCC and non-HCC was investigated. Magnified gel images and 3D views of two gp96 spots in non-HCC (A) and HCC (B) were shown. Differences in expression level of two gp96 spots, #436 (C) and #537 (D), between non-HCC and HCC were shown. The open circle indicates the standardized abundance of the individual spot in each sample. The closed square represents the averaged abundance of each gp96 spot. Magnified gel images of non-HCC (E) and HCC (F) stained with ProQ. The #436 spot was positively stained with ProQ, while unambiguous staining of the #537 spot was not observed. Tryptic peptides prepared from the spot #436 were analyzed by MALDI–TOF mass-spectrometry in the positive ion mode (G) and the negative ion mode (H). A peak of 2261.98 detected in positive ion mode corresponds to the amino acid sequence from 512 to 530. In addition to the original peak (*m/z*: 2260.53), a peak mass shifted by +80 Da was detected in the negative ion mode. A predicted phosphorylation consensus motif for protein kinase CK2 is indicated in italics (G).

ular chaperone and intracellular Ca^{2+} regulator [29,30]. Several previous reports have shown that gp96 is glycosylated and phosphorylated, and exists as heterogeneous molecular entities with various molecular weights [31]. In order to know whether gp96 spots were phosphorylated or not, we stained the 2-DE gels with ProQ Diamond which is a dye specific to proteins phosphorylated on serine, threonine or tyrosine residues [32], and has been used successfully to visualize phosphoproteins [33]. We found that the spot #436 was positively stained with ProQ (Fig. 3E and F). We further tried to detect possible phosphorylated peptides in the tryptic digests prepared from #436 by MALDI–TOF–MS according to Nabetani et al. [21]. Searching for those peaks that had relatively stronger intensities in negative ion mode than in positive ion mode, we found two peaks as candidates for acidically modified peptides. They were assigned to the peptides SILFVPTSAPR (amino acid sequence: 385–395, data not shown) and FQSSHHPTDITSLDQYVER (aa512–530). Fig. 3G and H show the unmodified peak and the acidically modified peak (mass shifted by +80 Da in negative ion mode) of the latter peptide, respectively. This peptide contained a predicted phosphorylation consensus motif, [Ser or Thr]-X-X-[Asp or Glu], for protein kinase CK2 (Fig. 3G) which was suggested to phosphorylate gp96 [34]. These results together with ProQ staining indicated that at least one gp96 isoform was phosphorylated and was up-regulated in HCC. Over-expression of gp96 in HCC has been reported previously [35], though the reports that showed over-expression of its phosphorylated form are rare. Further investigation into biological meaning of gp96 phosphorylation may provide us important information about HCC development.

Acknowledgments

We thank the late Dr. A. Tsugita for helpful discussion through this work and N. Tetsura for technical assistance.

Appendix A. Supplementary data

Supplementary data associated with this article can be found, in the online version, at doi:10.1016/j.bbrc.2007.11.101.

References

[1] T.K. Seow, R.C.M.Y. Liang, C.K. Leow, M.C.M. Chung, Hepatocellular carcinoma: from bedside to proteomics, Proteomics 1 (2001) 1249–1263.

[2] L.J. Lopez, J.A. Marrero, Hepatocellular carcinoma, Curr. Opin. Gastroenterol. 3 (2004) 248–253.

[3] H.F. Kawai, S. Kaneko, M. Honda, Y. Shirota, K. Kobayashi, Alpha-fetoprotein-producing hepatoma cell lines share common expression profiles of genes in various categories demonstrated by cDNA microarray analysis, Hepatology 3 (2001) 676–691.

[4] N. Iizuka, M. Oka, H. Yamada-Okabe, N. Mori, T. Tamesa, T. Okada, N. Takemoto, K. Hashimoto, et al., Differential gene expression in distinct virologic types of hepatocellular carcinoma: association with liver cirrhosis, Oncogene 22 (2003) 3007–3014.

[5] T. Yamashita, S. Kaneko, S. Hashimoto, T. Sato, S. Nagai, N. Toyoda, T. Suzuki, K. Kobayashi, et al., Serial analysis of gene expression in chronic hepatitis C and hepatocellular carcinoma, Biochem. Biophys. Res. Commun. 282 (2001) 647–654.

[6] K. Kawaguchi, M. Honda, T. Yamashita, Y. Shirota, S. Kaneko, Differential gene alteration among hepatoma cell lines demonstrated by cDNA microarray-based comparative genomic hybridization, Biochem. Biophys. Res. Commun. 329 (2005) 370–380.

[7] Y. Midorikawa, M. Makuuchi, W. Tang, H. Aburatani, Microarray-based analysis for hepatocellular carcinoma: from gene expression profiling to new challenges, World J. Gastroenterol. 13 (2007) 1487–1492.

[8] N.A. Shackel, D. Seth, P.S. Haber, M.D. Gorrell, G.W. McCaughan, The hepatic transcriptome in human liver disease, Comp. Hepatol. 5 (6) (2006).

[9] T.J. Griffin, S.P. Gygi, T. Ideker, B. Rist, J. Eng, L. Hood, R. Aebersold, Complementary profiling of gene expression at the transcriptome and proteome levels in *Saccharomyces cerevisiae*, Mol. Cell. Proteomics 4 (2002) 323–333.

[10] S.P. Gygi, Y. Rochon, B.R. Franza, R. Aebersold, Correlation between protein and mRNA abundance in yeast, Mol. Cell. Biol. 19 (1999) 1720–1730.

[11] M. Unlu, M.E. Morgan, J.S. Minden, Difference gel electrophoresis: a single gel method for detecting changes in protein extracts, Electrophoresis 11 (1997) 2071–2077.

[12] I.N. Lee, C.H. Chen, J.C. Sheu, H.S. Lee, G.T. Huang, C.Y. Yu, F.J. Lu, L.P. Chow, Identification of human hepatocellular carcinoma-related biomarkers by two-dimensional difference gel electrophoresis and mass spectrometry, J. Proteome Res. 6 (2005) 2062–2069.

[13] C.R. Liang, C.K. Leow, J.C. Neo, G.S. Tan, S.L. Lo, J.W. Lim, T.K. Seow, P.B. Lai, et al., Proteome analysis of human hepatocellular carcinoma tissues by two-dimensional difference gel electrophoresis and mass spectrometry, Proteomics 5 (2005) 2258–2271.

[14] V.J. Desmet, M. Gerber, J.H. Hoofnagle, M. Manns, P.J. Scheuer, Classification of chronic hepatitis: diagnosis, grading and staging, Hepatology 19 (1994) 1513–1520.

[15] K.G. Ishak, P.P. Anthony, L.H. Sobin, Histological typing of tumours of the liver, 2nd ed.WHO International Histological Classification of Tumors, Springer-Verlag, New York, 1994.

[16] M. Honda, S. Kaneko, H. Kawai, Y. Shirota, K. Kobayashi, Differential gene expression between chronic hepatitis B and C hepatic lesion, Gastroenterology 120 (2001) 955–966.

[17] H.F. Kawai, S. Kaneko, M. Honda, Y. Shirota, K. Kobayashi, Alpha-fetoprotein-producing hepatoma cell lines share common expression profiles of genes in various categories demonstrated by cDNA microarray analysis, Hepatology 33 (2001) 676–691.

[18] M. Honda, H. Kawai, Y. Shirota, T. Yamashita, T. Takamura, S. Kaneko, cDNA microarray analysis of autoimmune hepatitis, primary biliary cirrhosis and consecutive disease manifestation, J. Autoimmun. 25 (2005) 133–140.

[19] M. Honda, T. Yamashita, T. Ueda, H. Takatori, R. Nishino, S. Kaneko, Different signaling pathways in the livers of patients with chronic hepatitis B or chronic hepatitis C, Hepatology 44 (2006) 1122–1138.

[20] Y. Tabuse, T. Nabetani, A. Tsugita, Proteomic analysis of protein expression profiles during *Caenorhabditis elegans* development using 2D-difference gel electrophores, Proteomics 5 (2005) 2876–2891.

[21] T. Nabetani, K. Miyazaki, Y. Tabuse, A. Tsugita, Analysis of acidic peptides with a matrix-assisted laser desorption/ionization mass spectrometry using positive and negative ion modes with additive monoammonium phosphate, Proteomics 6 (2006) 4456–4465.

[22] Y. Kuramitsu, T. Harada, M. Takashima, Y. Yokoyama, I. Hidaka, N. Iizuka, T. Toda, M. Fujimoto, et al., Increased expression and phosphorylation of liver glutamine synthetase in well-differentiated

hepatocellular carcinoma tissues from patients infected with hepatitis C virus, Electrophoresis 27 (2006) 1651–1658.
[23] L. Hu, S.H. Lau, C.H. Tzang, J.M. Wen, W. Wang, D. Xie, M. Huang, Y. Wang, et al., Association of Vimentin overexpression and hepatocellular carcinoma metastasis, Oncogene 23 (2004) 298–302.
[24] Z. Dai, Y.K. Liu, J.F. Cui, H.L. Shen, J. Chen, R.X. Sun, Y. Zhang, X.W. Zhou, Identification and analysis of altered alpha1,6-fucosylated glycoproteins associated with hepatocellular carcinoma metastasis, Proteomics 6 (2006) 5857–5867.
[25] E. Zeindl-Eberhart, S. Haraida, S. Liebmann, P.R. Jungblut, S. Lamer, D. Mayer, G. Jäger, S. Chung, H.M. Rabes, Detection and identification of tumor-associated protein variants in human hepatocellular carcinomas, Hepatology 39 (2004) 540–549.
[26] W.H. Kuo, W.L. Chiang, S.F. Yang, K.T. Yeh, C.M. Yeh, Y.S. Hsieh, S.C. Chu, The differential expression of cytosolic carbonic anhydrase in human hepatocellular carcinoma, Life Sci. 73 (2003) 2211–2223.
[27] P.N. Cheng, T.L. Lam, W.M. Lam, S.M. Tsui, A.W. Cheng, W.H. Lo, Y.C. Leung, Pegylated recombinant human arginase (rhArgpeg5,000mw) inhibits the in vitro and in vivo proliferation of human hepatocellular carcinoma through arginine depletion, Cancer Res. 67 (2007) 309–317.
[28] F.S. Berven, O.A. Karisen, J.C. Murrell, H.B. Jensen, Multiple polypeptide forms observed in two-dimensional gels of Methylococcus capsulatus (Bath) polypeptides are generated during the separation procedure, Electrophoresis 24 (2003) 757–761.
[29] J. Melnick, S. Aviel, Y. Argon, The endoplasmic reticulum stress protein GRP94, in addition to BiP, associates with unassembled immunoglobulin chains, J. Biol. Chem. 267 (1992) 21303–21306.
[30] H. Liu, E. Miller, B. van de Water, J.L. Stevens, Endoplasmic reticulum stress proteins block oxidant-induced Ca^{2+} increases and cell death, J. Biol. Chem. 273 (1998) 12858–12862.
[31] A.M. Feldweg, P.K. Srivastava, Molecular heterogeneity of tumor rejection antigen/heat shock protein GP96, Int. J. Cancer 63 (1995) 310–314.
[32] T.H. Steinberg, B.J. Agnew, K.R. Gee, W.-Y. Leung, T. Goodman, B. Schulenberg, J. Hendrickson, J.M. Beechem, R.P. Haugland, W.F. Patton, Global quantitative phosphoprotein analysis using multiplexed proteomics technology, Proteomics 3 (2003) 1128–1144.
[33] B.R. Chitteti, Z. Peng, Proteome and phosphoproteome dynamic change during cell dedifferentiation in Arabidopsis, Proteomics 7 (2007) 1473–1500.
[34] S.E. Cala, GRP94 hyperglycosylation and phosphorylation in Sf21 cells, Biochim. Biophys. Acta 1496 (2000) 296–310.
[35] D.F. Yao, X.H. Wu, X.Q. Su, M. Yao, W. Wu, L.W. Qiu, L. Zou, X.Y. Meng, Abnormal expression of HSP gp96 associated with HBV replication in human hepatocellular carcinoma, Hepatobiliary Pancreat. Dis. Int. 5 (2006) 381–386.

ELSEVIER

Journal of Hepatology 50 (2009) 100–110

Journal of Hepatology

www.elsevier.com/locate/jhep

Activation of lipogenic pathway correlates with cell proliferation and poor prognosis in hepatocellular carcinoma☆

Taro Yamashita[1], Masao Honda[1,2], Hajime Takatori[1], Ryuhei Nishino[1], Hiroshi Minato[3], Hiroyuki Takamura[4], Tetsuo Ohta[4], Shuichi Kaneko[1,*]

[1]*Department of Gastroenterology, Kanazawa University Graduate School of Medical Science, 13-1 Takara-Machi, Kanazawa 920-8641, Japan*
[2]*Department of Advanced Medical Technology, Kanazawa University School of Health Sciences, 13-1 Takara-Machi, Kanazawa 920-8641, Japan*
[3]*Pathology Section, Kanazawa University Hospital, 13-1 Takara-Machi, Kanazawa 920-8641, Japan*
[4]*Department of Gastroenterologic Surgery, Kanazawa University Graduate School of Medical Science, 13-1 Takara-Machi, Kanazawa 920-8641, Japan*

***Background/Aims*: Metabolic dysregulation is one of the risk factors for the development of hepatocellular carcinoma (HCC). We investigated the activated metabolic pathway in HCC to identify its role in HCC growth and mortality.**

***Methods*: Gene expression profiles of HCC tissues and non-cancerous liver tissues were obtained by serial analysis of gene expression. Pathway analysis was performed to characterize the metabolic pathway activated in HCC. Suppression of the activated pathway by RNA interference was used to evaluate its role in HCC *in vitro*. Relation of the pathway activation and prognosis was statistically examined.**

***Results*: A total of 289 transcripts were up- or down-regulated in HCC compared with non-cancerous liver ($P < 0.005$). Pathway analysis revealed that the lipogenic pathway regulated by sterol regulatory element binding factor 1 (*SREBF1*) was activated in HCC, which was validated by real-time RT-PCR. Suppression of *SREBF1* induced growth arrest and apoptosis whereas overexpression of *SREBF1* enhanced cell proliferation in human HCC cell lines. *SREBF1* protein expression was evaluated in 54 HCC samples by immunohistochemistry, and Kaplan–Meier survival analysis indicated that *SREBF1*-high HCC correlated with high mortality.**

***Conclusions*: The lipogenic pathway is activated in a subset of HCC and contributes to cell proliferation and prognosis.**

***Keywords*: Hepatocellular carcinoma; Serial analysis of gene expression; Lipogenesis; Gene expression profiling; Sterol regvulatory element binding factor 1**

Received 26 May 2008; received in revised form 1 July 2008; accepted 23 July 2008; available online 12 October 2008
Associate Editor: J.M. Llovet

☆ The authors who have taken part in the research of this paper declared that they do not have a relationship with the manufacturers of the materials involved either in the past or present and they did not receive funding from the manufacturers to carry out their research.

* Corresponding author. Tel.: +81 76 265 2231; fax: +81 76 234 4250.
E-mail address: skaneko@m-kanazawa.jp (S. Kaneko).

Abbreviations: HCC, hepatocellular carcinoma; *SREBF1*, sterol regulatory element binding factor 1; HBV, hepatitis B virus; HCV, hepatitis C virus; SAGE, serial analysis of gene expression; RT-PCR, reverse transcription-polymerase chain reaction; IHC, immunohistochemistry; FADS1, fatty acid desaturase 1; SCD, stearoyl CoA desaturase; FASN, fatty acid synthase; si-RNA, short interfering-RNA; CLD, chronic liver disease; PCNA, proliferating cell nuclear antigen; IGF, insulin-like growth factor.

1. Introduction

Hepatocellular carcinoma (HCC) is one of the most frequently occurring malignancies in the world [1]. The major risk factors associated with HCC include chronic infection with hepatitis B virus (HBV) and hepatitis C virus (HCV), alcohol abuse, and exposure to aflatoxin B1 [2]. HCC usually develops from liver cirrhosis, which involves continuous inflammation and hepatocyte regeneration, suggesting that reactive oxygen species and DNA damage are involved in the process of hepatocarcinogenesis [3].

The development of gene expression profiling technologies including DNA microarrays and serial analysis

0168-8278/$34.00
doi:10.1016/j.jhep.2008.07.036

of gene expression (SAGE) have enhanced our ability to identify inventory transcripts and global genetic alterations in HCC [4–10]. In general, these methods have demonstrated that transcripts associated with cell growth are up-regulated, whereas those related to inhibition of cell growth are down-regulated, in HCC [11]. It is difficult, however, to decipher molecular pathways activated during hepatocarcinogenesis.

Epidemiological studies suggest that metabolic dysregulation in the liver increases the risk of HCC development. For example, diabetes is associated with a 2-fold increase in the risk of HCC [12]. Obesity and hepatic steatosis also increase the risk of HCC [13–15]. Furthermore, recent studies indicate that HCV infection provokes hepatic steatosis, which may be a vulnerable factor for liver inflammation and HCC development [16,17]. Thus, dysregulation of a metabolic pathway may play a crucial role to promote HCC growth, but the molecular mechanism is still obscure. In this study, we have utilized SAGE [18,19], which enables us to monitor the differential expression of all genes, to determine the global changes in gene expression that occur during hepatocarcinogenesis.

2. Materials and methods

2.1. Tissue samples

All HCC tissues, adjacent non-cancerous liver tissues, and normal liver tissues were obtained from 69 patients who underwent hepatectomy from 1997 to 2005 in Kanazawa University Hospital. Normal liver tissue samples were obtained from patients undergoing surgical resection of the liver for treatment of metastatic colon cancer. HCC and surrounding non-cancerous liver samples were obtained from patients undergoing surgical resection of the liver for the treatment of HCC. The samples used for SAGE, real-time reverse-transcription (RT)-PCR analysis, and immunohistochemistry (IHC) are listed in Supplemental Table 1. All samples used for SAGE and real-time RT-PCR analysis were snap-frozen in liquid nitrogen. Four normal liver tissues and 20 HCCs and their corresponding non-cancerous liver tissues were used for real-time RT-PCR analysis; seven of these HCC samples, along with 47 additional HCC samples, were formalin-fixed paraffin-embedded and used for IHC. HCC and adjacent non-cancerous liver were histologically characterized as described [20].

All strategies used for gene expression analysis as well as tissue acquisition processes were approved by the Ethics Committee and the Institutional Review Board of Kanazawa University Hospital. All procedures and risks were explained verbally, and each patient provided written informed consent.

2.2. SAGE

Total RNA was purified from each homogenized tissue sample using a ToTally RNA extraction kit (Ambion, Inc., Austin, TX), and polyadenylated RNA was isolated using a MicroPoly (A) Pure kit (Ambion). A total of 2.5 μg mRNA per sample was analyzed by SAGE [18]. SAGE libraries were randomly sequenced at the Genomic Research Center (Shimadzu-Biotechnology, Kyoto, Japan), and the sequence files were analyzed with SAGE 2000 software. The size of each SAGE library was normalized to 300,000 transcripts per library, and the abundance of transcripts was compared by SAGE 2000 software. Monte Carlo simulation was used to select genes with significant differences in expression between two libraries without multiple hypothesis testing correction ($P < 0.005$) [21]. Each SAGE tag was annotated using a gene-mapping web site (http://www.ncbi.nlm.nih.gov/SAGE/index.cgi).

2.3. Analysis of signaling networks

Ingenuity Pathways Analysis software (Ingenuity® Systems, www.ingenuity.com) was used to investigate the molecular pathways activated in an HCC SAGE library compared with an adjacent non-cancerous liver SAGE library. All reliable transcripts statistically up-regulated in HCC were investigated and annotated with biological processes, protein-protein interactions, and gene regulatory networks, using a reference-based data file with statistical significance. All identified pathways were screened individually. MetaCore™ software (GeneGo Inc., St. Joseph, MI) was used to evaluate candidate transcription factors responsible for up-regulation of transcripts in HCC.

2.4. RT-PCR

A 1-μg aliquot of each total RNA was reverse-transcribed using SuperScript II reverse-transcriptase (Invitrogen, Carlsbad, CA). Real-time RT-PCR analysis was performed using ABI PRISM 7900 Sequence Detection System (Applied Biosystems, Foster City, CA). Using the standard curve method, quantitative **PCR** was performed in triplicate for each sample-primer set. Each sample was normalized relative to β-actin. The assay IDs used were Hs00231674_m1 for sterol regulatory element binding factor 1 (*SREBF1*); Hs00203685_m1 for fatty acid desaturase 1 (*FADS1*) ;Hs00748952_s1 for stearoyl CoA desaturase (*SCD*); Hs00188012_m1 for fatty acid synthase (*FASN*); and Hs99999_m1 for β-actin. *SREBF1a* and *SREBF1c* mRNA levels were assayed by semi-quantitative RT-PCR [22].

2.5. RNA Interference targeting SREBF1

Si-RNAs targeting *SREBF1* were constructed using a *Silencer*™ SiRNA Construction kit (Ambion) according to the manufacturer's protocol. We constructed two different si-RNAs, targeting different sites of *SREBF1* (*SREBF1*-1; CAGTGGCACTGACTCTTCC, *SREBF1*-2; TCTACGACCAGTGGGACTG). Control si-RNA duplexes targeting scramble sequences were also synthesized (Dharmacon Research, Inc., Lafayette, CO). Lipofectamine 2000™ reagent (Invitrogen) was used for transfection according to the manufacturer's instructions.

2.6. Cell proliferation assay

Cell proliferation assays were performed using a Cell Titer96 Aqueous kit (Promega, Madison, WI). Results are expressed as the mean optical density (OD) of each five-well set. All experiments were repeated at least twice.

2.7. Soft agar assay

To each well of a six-well plate, containing a base layer of 0.72% agar in growth medium, was added 1×10^4 cells, suspended in 2 ml of 0.36% agar with growth medium (DMEM supplemented with 10% FBS), and the plates were incubated at 37 °C in a 5% CO_2 incubator for 2 weeks. The numbers of colonies in each well were counted as previously described [23].

2.8. TUNEL assay

A DeadEnd™ Colorimetric TUNEL System (Promega) was used to measure nuclear DNA fragmentation as described previously [24].

2.9. Annexin V staining

To evaluate apoptotic cell death, Annexin V binding to cell membranes was evaluated using Annexin V-FITC antibodies and FACSCalibur flow cytometer (BD Biosciences, Franklin Lakes, NJ), as described by the manufacturer.

2.10. Focus assay

HuH7 cells and Hep3B cells were transiently transfected with pCMV7 or pCMV7-*SREBF1c* vectors (kindly provided by Dr. Hitoshi Shimano) using Lipofectamine 2000™ reagent (Invitrogen), as described by the manufacturer. A total of 2×10^3 cells were seeded on six-well plates 48 h after transfection, and cultured in usual media with 400 ng/ml of Geneticin for 9 days. The foci were fixed with ice-cold 100% methanol and stained with 0.5% crystal violet solution. All experiments were performed in triplicates.

2.11. Western blotting

Whole cell lysates were prepared using RIPA lysis buffer. Antibodies used were rabbit polyclonal antibodies to phospho-GSK-3β (ser9) (Cell Signaling Technology Inc., Danvers, MA), rabbit anti-sterol regulatory element binding protein-1 (encoded by *SREBF1*) polyclonal antibody H-160 (Santa Cruz Biotechnology, Inc., Santa Cruz, CA), and β-actin (Sigma–Aldrich Japan K.K., Tokyo, Japan). Immune complexes were visualized by enhanced chemiluminescence (Amersham Biosciences Corp., Piscataway, NJ) as described in the manufacturer's protocol.

2.12. Immunohistochemistry

Rabbit anti-*SREBF1* polyclonal antibody H-160 (Santa Cruz Biotechnology, Inc.) and mouse anti-proliferating cell nuclear antigen (PCNA) monoclonal antibody PC10 (Calbiochem, San Diego, CA) were used to evaluate the immunoreactivity of HCC samples, using a DAKO EnVision+™ Kit, as described by the manufacturer. The signal intensity of *SREBF1* was scored as negative, low, or high determined by the representative staining of the normal liver tissue and cirrhotic liver tissue (Supplemental Fig. 1). HCC was referred as *SREBF1*-high if *SREBF1* expression in the tumor was higher than that in the cirrhotic liver tissue. PCNA index was evaluated as previously described [25].

2.13. Statistical analysis

Kruskal–Wallis test was used to compare the differentially expressed genes, as shown by real-time PCR, among normal liver, CLD, and HCC tissues. Mann–Whitney U test was also used to evaluate the statistical significance of differences of gene expression between CLD and HCC tissues. Spearman's correlation coefficient was used to assess correlations between the expression levels of *SREBF1*, *FADS1*, *SCD*, and *FASN*. Univariate Cox proportional hazards regression analysis was used to evaluate the association of gene expression and clinicopathologic parameters with patient outcomes. All statistical analyses were performed using SPSS software (SPSS software package; SPSS Inc., Chicago, IL) and GraphPad Prism software (GraphPad Software Inc., La Jolla, CA).

3. Results

3.1. Gene expression profiling of HCC

We constructed two SAGE libraries from a HCC–HBV tissue and a corresponding non-cancerous tissue (chronic liver disease (CLD)–HBV). We also used two previously described SAGE libraries, from an HCC–HCV sample and a corresponding non-cancerous tissue sample (CLD–HCV) [4]. After excluding tags detected only once in each library, to avoid the contamination of tags derived from sequence errors, we selected 105,288 tags corresponding to the 9731 genes in all libraries. Using Monte Carlo simulation, we compared the differentially expressed transcripts in HCC and corresponding CLD libraries. Compared with their corresponding CLD libraries, there were statistically significant increases or decreases in 140 transcripts in the HCC–HBV library and in 197 transcripts in the HCC–HCV library ($P < 0.005$).

The HCC–HBV library contained one SAGE tag encoding the HBV–X region, which was increased more than 35-fold compared with its expression in the corresponding CLD–HBV library (Supplemental Table 2). We identified two additional SAGE tags, encoding unknown genes (GTTCTAAAGG, GCATTATGAT), which were expressed more than 10-fold in the HCC–HBV library than in the corresponding CLD–HBV library. The HCC–HBV library also contained tags associated with lipogenesis, at greater than 10-fold abundance, in the HCC–HBV library; these including tags for steroyl-CoA desaturase, fatty acid synthase, and fatty acid desaturase 1.

In contrast, SAGE tags associated with the immune response were up-regulated in the HCC–HCV library. These included tags for Th1-type chemokines, including chemokine ligand 10 (C–X–C motif), chemokine ligand 9 (C–X–C motif), and major histocompatibility complex classes IA and IB (Supplemental Table 3). In addition, tags associated with lipogenesis were increased in the HCC–HCV library, including tags for 3-hydroxy-3-methylglutaryl-coenzyme A synthase 1 and cytochrome P450, family 51, subfamily A, polypeptide 1. Taken together, the differential gene expression patterns may exist in HCC–HBV and HCC–HCV. HBV–X and lipogenesis-related genes are activated in HCC–HBV, whereas genes associated with inflammation as well as lipogenesis are activated in HCC–HCV.

3.2. Analysis of molecular pathways activated in HCC

To further characterize the gene expression patterns of HCC–HBV and HCC–HCV, we performed pathway analysis on SAGE data. Using MetaCore™ software, we found that the candidate transcription factors activated were distinct in each HCC library (Table 1). Several of these transcription factors, including NF-κB, c-Myc, c-Jun, and HNF4-α, have been reported to be activated in HCC [26–29]. In addition, our findings indicated that the transcription factor *SREBF1* may be activated in both HCC–HBV and HCC–HCV (to avoid a confusion, we use HUGO symbol *SREBF1* to indicate both gene/protein name).

Table 1
Candidate transcription factors that regulate molecular pathways activated in HCC.

SAGE library	Transcription factor	Molecular processes	*P*-value
HCC–HCV	NF-κB	Antigen presentation Antigen processing Defense response Immune response	0.004
	SREBF1	Cholesterol biosynthesis Lipid biosynthesis β-Glucoside transport Negative regulation of lipoprotein metabolism	0.05
	SP1	Electron transport; drug metabolism Oxygen and reactive oxygen species metabolism Cell-substrate junction assembly; wound healing	0.05
	IRF1	Immune response Antigen presentation; antigen processing Defense response; positive regulation of cell	0.05
HCC–HBV	HNF4-α	Lipid transport Fatty acid metabolism Smooth muscle cell proliferation	0.002
	HNF1	Acute-phase response; lipid transport Negative regulation of lipid catabolism β-Glucoside transport Negative regulation of lipoprotein metabolism	0.01
	SP1	Zinc ion homeostasis; response to biotic stimulus Nitric oxide mediated signal transduction Copper ion homeostasis; fatty acid biosynthesis	0.01
	c-Jun	Progesterone catabolism; progesterone metabolism Regulation of lipid metabolism; Prostaglandin metabolism	0.03
	C/EBP-α	Lipid transport; negative regulation of lipid catabolism Negative regulation of lipoprotein metabolism β-Glucoside transport Positive regulation of interleukin-8 biosynthesis	0.03
	SREBF1	Lipid biosynthesis; fatty acid biosynthesis Fatty acid metabolism Negative regulation of lipid catabolism Negative regulation of lipoprotein metabolism	0.03
	c-Myc	Fatty acid biosynthesis; fatty acid metabolism Fatty acid desaturation; Activation of pro-apoptotic gene products Release of cytochrome c from mitochondria	0.03
	USF1	Fatty acid metabolism Smooth muscle cell proliferation	0.03
	PPAR-α	Fatty acid metabolism Smooth muscle cell proliferation	0.03
	COUP-TFI	Lipid transport Smooth muscle cell proliferation	0.03
	C/EBP-β	Acute-phase response Regulation of interleukin-6 biosynthesis Fat cell differentiation Inflammatory response	0.03

These findings were evaluated by other pathway analysis software, Ingenuity Pathways Analysis (IPA). We applied the signaling network analysis to the transcripts up-regulated in the HCC libraries ($P < 0.005$). We found that the top signaling network activated in HCC–HBV contained several pathways involved in ERK/MAPK signaling, PPAR signaling, linoleic acid metabolism, and fatty acid metabolism (Supplemental Fig. 2A). Similarly, pathways involved in interferon signaling, NF-κB signaling, antigen presentation, PPAR signaling, linoleic acid metabolism, and fatty acid metabolism were included in the top signaling network activated in HCC–HCV (Supplemental Fig. 2B). Consistent with the results of transcription factor analysis by MetaCore™, pathway analysis indicated that *SREBF1* participates in the lipogenesis pathway in both HCC–HBV and HCC–HCV (blue nodes in Supplemental Fig. 2A and B). *SREBF1*, a major regulator of the lipogenesis pathway, binds to sterol regulatory elements on the genome [30], but less is known about its role in

HCC [31]. We therefore focused on the role of *SREBF1* signaling in HCC.

3.3. Validation of SAGE and signaling network analysis

We performed real-time RT-PCR analysis of *SREBF1* and three representative target genes (*SCD*, *FADS1*, and *FASN*) [20] on 44 samples not used for SAGE. We found that the levels of *SREBF1*, *SCD*, and *FASN* mRNAs were higher in HCC tissues and CLD tissues compared with normal liver, and that these differences were statistically significant (Fig. 1A). We further compared the expression of *SREBF1*, *FADS1*, and *FASN* between HCC and non-cancerous liver tissues, and identified the overexpression of *SREBF1* in HCC with statistical significance (Supplemental Fig. 3). Scatter plot analysis showed that the expression levels of *SREBF1* were correlated with those of *FADS1* ($R = 0.57$, $P < 0.0001$), *SCD* ($R = 0.82$, $P < 0.0001$), and *FASN* ($R = 0.74$, $P < 0.0001$) (Fig. 1B).

Since the mammalian genome encodes two *SREBF1* isoforms, *SREBF1a* and *SREBF1c* [22], we performed semi-quantitative RT-PCR with isoform specific primers to determine which of these isoforms was up-regulated in HCC. We found that *SREBF1c* mRNA, but not *SREBF1a* mRNA, was up-regulated in HCC compared with adjacent non-cancerous liver and normal liver tissues (Supplemental Fig. 4A).

3.4. Functional assay of the lipogenesis pathway in cell lines

Although genome-wide expression profiling showed that the lipogenesis pathway was activated in HCC possibly through up-regulation of *SREBF1*, it was not clear that this pathway played a role in HCC growth. To investigate the role of lipogenesis in HCC cell proliferation, we transfected two short interfering (si)-RNAs (*SREBF1*-1 and *SREBF1*-2) targeting *SREBF1* into the HuH7 and Hep3B cells. These cell lines have no chromosome amplification or deletion on 17p11, on which *SREBF1* is located [32]. Transfection of the si-RNA constructs for *SREBF1*-1 or *SREBF1*-2 decreased expression of *SREBF1* 90% and 70%, respectively, and the expression of both *SCD* and *FADS1* 70% and 60%, respectively (Fig. 2A). Because differences in *SREBF1c* and *SREBF1a* *sequence alignments* are very small, we could not design si-RNAs specifically targeting *SREBF1c*. We therefore checked the effect of si-RNAs on the expression of the *SREBF1* isoforms. We found that the expression of *SREBF1c* was relatively more suppressed than that of *SREBF1a* (Supplemental Fig. 4B), which may have been associated with the higher expression of *SREBF1a* than *SREBF1c* in cultured cell lines [25].

We found that the growth of these transfected cells was significantly inhibited at 72 h compared with mock transfected cells (Fig. 2B and Supplemental Fig.5A). Examination of anchorage independent cell growth showed strong suppression by deactivation of the lipogenesis pathway (Fig. 2C). Because insulin-like growth factor (IGF) is known to induce cancer cell proliferation through activation of PI3-kinase signaling followed by *SREBF1* induction, we investigated the effect of *SREBF1* knockdown on IGF2 mediated cell proliferation. Interestingly, *SREBF1* knockdown abrogated the IGF2 dependent cell proliferation (Supplemental Fig. 5B). Moreover, both the TUNEL assay and annexin V staining showed that transfection of *SREBF1* si-RNAs increased apoptosis compared with mock transfected cells (Fig. 2D and E).

We further investigated the role of *SREBF1* overexpression on cell growth *in vitro*. We transiently transfected control pCMV7 plasmids or pCMV7-*SREBF1c* plasmids (Fig. 3A), and cell proliferation was enhanced in *SREBF1* overexpressing cells compared with the control in both HuH7 and Hep3B cells evaluated by focus assay (Fig. 3B and supplemental Fig. 6). Furthermore, overexpression of *SREBF1* intensified the phosphorylation of GSK-3β, one of the major kinase phosphorylated by the activation of IGF signaling, in a dose-dependent manner (Fig. 3C).

3.5. SREBF1 Expression and prognosis

Since the above results indicated that *SREBF1* signaling may play an important role on tumor cell growth, we investigated the relationship between *SREBF1* expression and mortality in 54 HCC patients by IHC. When we examined the expression of *SREBF1* in HCC tissues and adjacent non-cancerous liver tissues, we identified the increase of the cytoplasmic *SREBF1* staining in a subset of HCC (Fig. 4A). We evaluated the expression of *SREBF1* in HCC and classified 4, 30, and 20 HCCs as *SREBF1*-negative, *SREBF1*-low, and *SREBF1*-high HCC, respectively (Fig. 4B and Supplemental Fig. 1). We could not detect any differences of clinico-pathological characteristics between *SREBF1*-high HCC and *SREBF1*-low/-negative HCC including histological steatosis (Supplemental Table4). Since the seven of these HCC samples were also used for real-time RT-PCR analysis, we investigated the relation of *SREBF1* RNA and protein expression (Fig. 4C). *SREBF1*RNA expression was significantly higher in *SREBF1*-high HCC than in *SREBF1*-low/-negative HCC with statistical significance ($P = 0.03$). Then we examined the cell proliferation of these HCC samples by PCNA staining. Notably, PCNA indexes were significantly higher in *SREBF1*-high HCC than *SREBF1*-low/-negative HCC with statistical significance ($P < 0.001$) (Fig. 4D). We further investigated the relationship between *SREBF1*

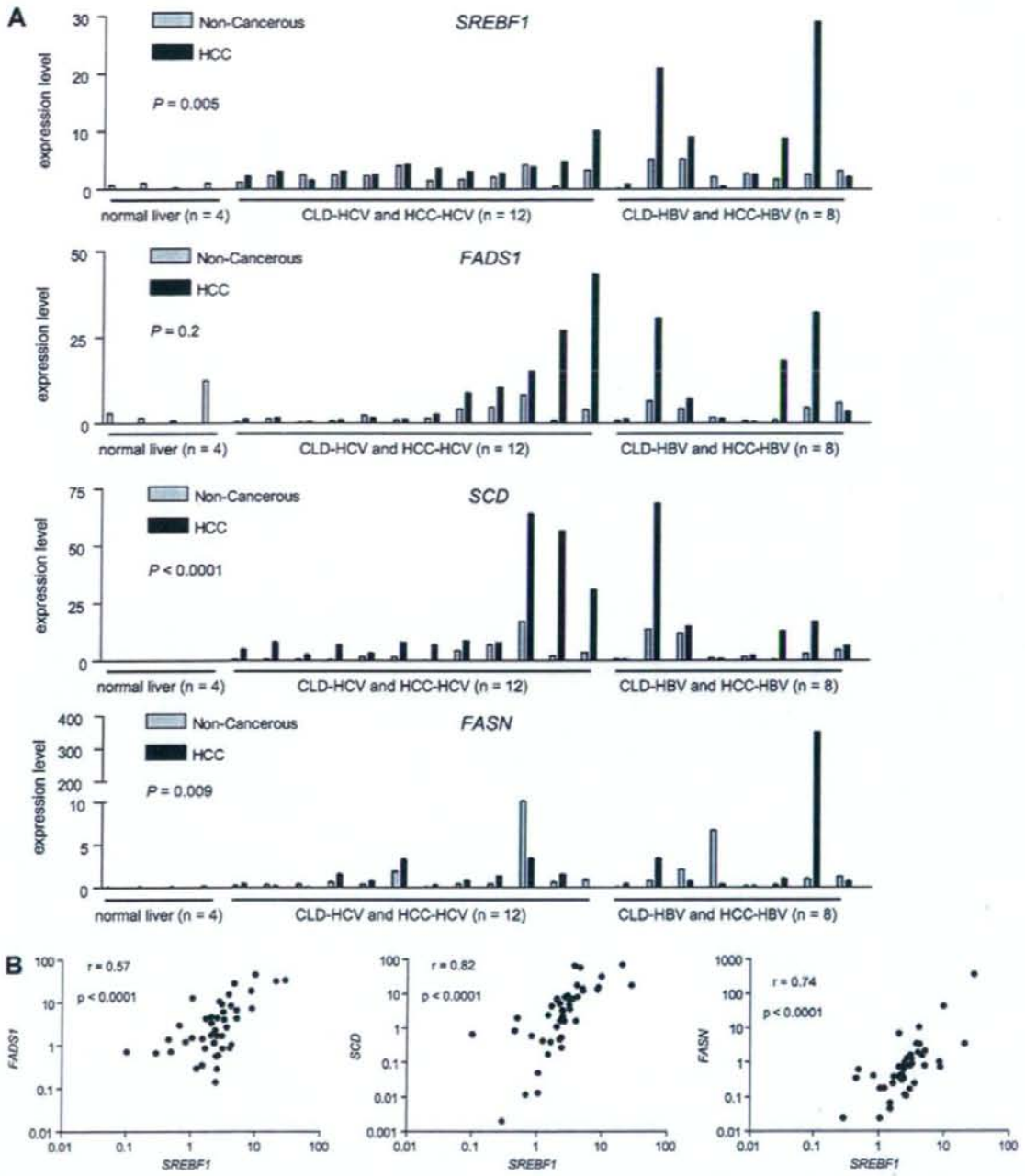

Fig. 1. (A) Real-time quantitative RT-PCR analysis. RNA was isolated from 44 tissue samples: 20 HCC, 20 corresponding CLD, and four normal liver samples. Differential expression of each gene among normal liver tissues, CLD tissues, and HCC tissues was examined by Kruskal–Wallis tests. (B) Scatter plot analysis. Gene expression levels of *FADS1*, *SCD* and *FASN* were well-correlated with those of *SREBF1*, as shown by Spearman's correlation coefficients.

protein expression and prognosis. Kaplan–Meier survival analysis showed a significant relationship between poor survival and high *SREBF1* protein expression ($P = 0.04$; Fig. 4E). Univariate Cox regression analysis showed a correlation between high *SREBF1* protein expression and high risk of mortality with statistical